

ELECTRON COOLING STATUS AND CHARACTERIZATION AT FERMILAB'S RECYCLER*

L.R. Prost[#], A. Burov, K. Carlson, A. Shemyakin, M. Sutherland, A. Warner, FNAL, Batavia, IL 60510, U.S.A.

Abstract

FNAL's electron cooler (4.3 MV, 0.1 A DC) has been integrated to the collider operation for almost two years, improving the storage and cooling capability of the Recycler ring (8 GeV antiprotons). In parallel, efforts are carried out to characterize the cooler and its cooling performance.

This paper discusses various aspects of the cooler performance and operational functionality: high voltage stability of the accelerator (Pelletron), quality of the electron beam generated, operational procedures (off-axis cooling, electron beam energy measurements and calibration) and cooling properties (in the longitudinal and transverse directions).

INTRODUCTION

The Recycler Electron Cooler (REC) [1] has been fully integrated to the collider operation since January 2005. However, over the past year, the average antiproton production rate in the Accumulator ring has almost doubled, reducing the average time between successive injections into the Recycler from 4 to 2.5 hours, hence increasing the need for fast cooling. In turn, the REC has been heavily relied upon for the storage and cooling of 8 GeV antiprotons destined for collisions in the Tevatron.

In this paper, we report on the status of the electron cooler, which has proved to be very reliable over the past year. We also discuss its overall cooling performance, through dedicated friction force and cooling rate measurements.

THE REC IN OPERATION

The REC employs a DC electron beam generated in an electrostatic accelerator, Pelletron [2], operated in the energy- recovery mode. The beam is immersed into a longitudinal magnetic field at the gun and in the cooling section (CS); other parts of the beam line use lumped focusing. The main parameters of the cooler can be found in Ref. [1].

Cooling Procedure

The cooling procedure described in Ref. [3] remains the norm to this date: the electron beam is used when needed and the cooling rate is being adjusted by increasing or decreasing the fraction of the antiproton beam that the electron beam overlaps (through parallel shifts). The driving consideration for this procedure is to avoid overcooling the center of the antiproton beam and

preserve its lifetime.

A cooling sequence is illustrated on Figure 1 and in this particular case the electron beam was turned on just before the 3rd injection (out of 11) and kept on until extraction to the Tevatron. Throughout the storage cycle, the electron beam position is adjusted regularly according to the needs for longitudinal cooling. Note that stochastic cooling is always on (both the longitudinal and transverse systems).

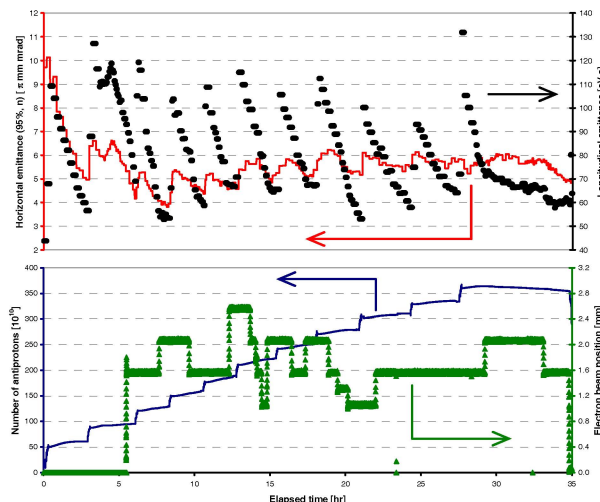


Figure 1: Example of the cooling sequence and electron beam utilization during a storage cycle. Bottom plot - Solid blue: Number of antiprotons; Green triangles: Electron beam position; Top plot - Solid red: Transverse (horizontal) emittance measured by the 1.75 GHz Schottky detector; Black circles: Longitudinal emittance measured by the 1.75 GHz Schottky detector. The electron beam current is kept constant (100 mA).

At the end of the storage cycle, just before mining [4], the beam is brought 'on-axis' (i.e. the electron beam trajectory coincides with the antiprotons central orbit) to provide maximum cooling when lifetime preservation is no longer an issue since the antiprotons are about to be extracted to the Tevatron. Recently, to accommodate the large number of particles often present in the Recycler ($>300 \times 10^{10}$), the electron beam current is increased from 100 mA to 200 mA after the last injection of fresh antiprotons. The additional cooling strength obtained from the increased beam current is required to reach the longitudinal emittance needed for high transfer efficiencies in the downstream machines all the way to collision in the Tevatron.

The final cooling sequence (between the last injection from the Accumulator to extraction to the Tevatron) takes 2-2h30 (Figure 2). It is dictated by the needs for reducing the longitudinal emittance from 110-120 eV s (just after

*Operated by Fermi Research Alliance, LLC under Contract No. DE-AC02-07CH11359 with the United States Department of Energy

[#]lprost@fnal.gov

the last injection) to 60-70 eV s before extraction to the Tevatron [5], while maintaining a decent beam lifetime (> 100 hours). However, in this case, cooling ultimately takes priority on lifetime preservation, although the cooling strength is increased in steps. On Figure 2, one can see how moving the electron beam closer to the antiprotons central orbit decreases both the longitudinal and transverse emittances but also affects the lifetime.

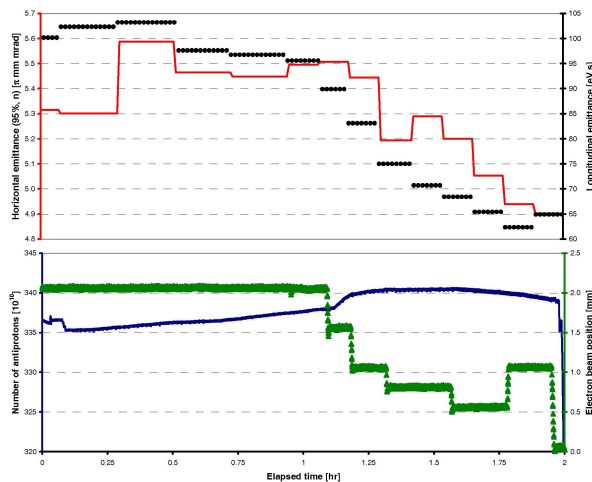


Figure 2: Example of a final cooling sequence. The legend is the same as for Figure 1. Electron beam is kept constant (200 mA).

The antiproton beam lifetime is currently difficult to extract quantitatively because the main beam current diagnostic, a DCCT, failed and the alternate beam current monitor does not perform reliably with the barrier-bucket RF structure. Nevertheless, the fact that the beam current signal turns over indicates a real degradation of the antiproton lifetime. Note that a new DCCT has been installed during our latest shutdown period, which will give us back the ability to investigate lifetime issues in the Recycler (induced or not by the presence of the electron beam).

Availability and Performance Stability

Due to the increased demand on electron cooling, it is imperative that the cooler be very reliable. A storage cycle (between extractions to the Tevatron) typically lasts 25-35 hours and, on average, the electron beam is used 75% of this time, with an electron current $I_b = 100$ -200 mA. During our recent run (\sim past 8 months), the number of downtimes needed for conditioning of the acceleration tubes was approximately once every two months. Conditioning usually followed a series (2-3) of full discharges, when the Pelletron voltage drops to zero in a sub- μ s time, and the pressure in one of the acceleration tubes increases by several orders of magnitude. When they occur, full discharges take 30-60 minutes to recover from while conditioning takes 4-8 hours. However, note that when possible, conditioning is carried out during times when the electron beam is not absolutely required, limiting its operational impact. In addition, routine maintenance requiring opening of the

Pelletron tank (\sim 3 days of downtime) were carried out once every 5-6 months, when the whole complex undergoes some downtime, mainly for cleaning of the charging circuitry (chain, pulleys, sheaves, corona needles replacement). Other sources of beam downtime were mostly related to issues with the controls system. Short recirculation interruptions (< 1 min with low impact on the operation performance) have also been sparse (\sim 2-10 per day) and many of them were false-positive due to losses from the Main Injector (i.e. proton loss during acceleration) being recorded by the electron cooler protection system. The latter has been resolved by masking (in the software) the Main Injector losses during acceleration.

Besides the intrinsic cooling performance to be discussed in the following section, being able to maintain (or quickly return to) optimum conditions for efficient cooling during operation is critical. The main three reasons that hinder the cooling performance were found to be the degradation of the cooling section magnetic field straightness, the antiproton trajectory drift and the Pelletron HV stability.

Once the electron beam trajectory has been optimized, we find that, over time, it changes in a fashion consistent with a degradation of the straightness of the magnetic field from solenoid to solenoid. To correct for this misalignment, a beam-based procedure was developed, relying on cooling rate and/or friction force measurements [6]. Over the past year, this procedure was repeated twice and the cooling efficiency increased both time.

While for storing purposes the antiproton trajectories only need to be stable to the ~ 1 mm level, for cooling purposes, any misalignment between the electron and antiproton beam trajectories introduces a shift and/or adds an effective angle which impacts the cooling performance. For reason not well determined (but ground motion is a possible candidate along with failing power supplies), we find that the antiproton beam trajectories need to be adjusted regularly, once every 1-2 months, or when a significant piece of hardware has been changed out (i.e. a corrector bulk power supply). To do so, a localized 3-bumps has been implemented, which allows for steering the antiproton beam in the cooling section both for its position and its average tilt, while maintaining a closed orbit around the ring.

Finally, the Pelletron high voltage stability may be the one parameter that can have a significant impact on operation in various ways.

First, the most detrimental events for the integrity of the cooler are the full discharges. Specific efforts to reduce their frequency are reported in Ref. [7,8]. As mentioned in the first section of this paper, during our recent run (\sim past 8 months), the number of full discharges was limited to \sim 2-3 every two months, with successive discharges typically occurring over a few days, at which point, conditioning of the tubes was undertaken. In all cases, the conditioning process revealed that the

weakened region was located in the top half of the acceleration tubes (low kinetic energy).

Then, besides high voltage events leading to beam interruptions, the question of the Pelletron energy stability (relative and absolute) arises. We found that the average energy of the electron beam drifts over long period of times (by up to 1-2 keV), which reduces greatly the cooling efficiency. In addition, it is sensitive to the Pelletron temperature and the energy changes at the rate of ~ -300 V/°C. This is mostly an issue at turn on since it takes 6-10 hours for the Pelletron to reach its equilibrium temperature. Figure 3 shows an example of the typical flattened antiproton longitudinal distribution measured with a Schottky pickup when the electron beam momentum is offset by some significant amount with respect to the antiproton momentum (left). For comparison, Figure 3 also shows the much sharper peak (right) that one obtains when the electron beam energy is close to being optimal. Although the antiproton momentum distribution is a good indication that the electron beam energy is not adequate *a posteriori*, it does not provide the magnitude and the sign of the mismatch.

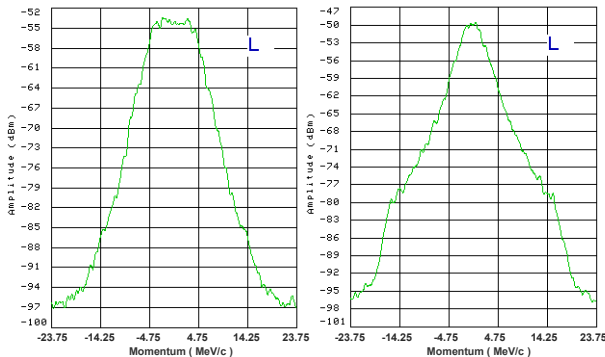


Figure 3: Antiproton longitudinal distributions measured with the 1.75 GHz Schottky detector. In both cases, the electron beam was on axis for ~ 2 h at 100 mA. Bunch length = 6.1 μ s. $N_p = 200 \times 10^{10}$ (left) and 280×10^{10} (right) particles.

The absolute electron beam energy calibration is done using un-bunched antiprotons (no RF structure) and measuring its longitudinal Schottky distribution, for which the frequency of the peak with respect to the revolution frequency indicates the absolute momentum shift between the two beams. However, this method can only be used with a very low number of antiprotons in the ring ($< 20 \times 10^{10}$) and does not allow for opportune checks. Instead, we are able to utilize the 180° bend magnet following the cooling section and a beam position monitor (BPM) just downstream (R01) as an energy analyzer. Again using antiprotons for calibration purposes, the absolute vertical (y) position is recorded, as well as the relative displacement of the beam as a function of the electron beam energy. Figure 4 shows the Pelletron's high voltage read back and the corresponding beam displacement at R01 when a step function is applied. While the relative calibration (0.31 mm/kV) is very

stable, the absolute position at R01 for a fixed energy does vary with time also and needs to be recalibrated with antiprotons \sim once a month. This is because the position at the entrance of the bend is not exactly fixed due to upstream drifts (BPM electronics, power supplies stability, ground motion).

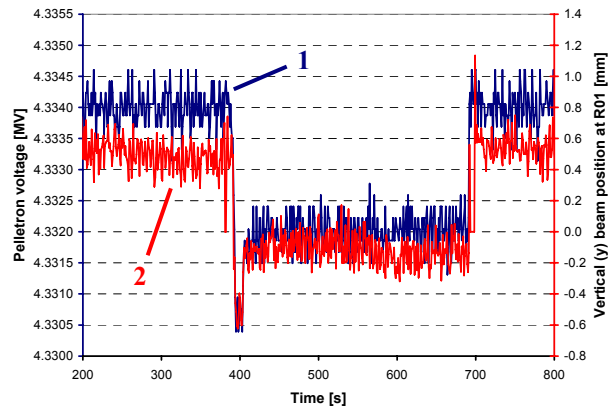


Figure 4: Pelletron voltage (1-blue) and electron beam vertical (y) position at R01 (2-red) as function of time during a voltage jump. The corresponding calibration is 0.31 mm/kV.

The use of the beam position at R01 as a measure of the electron beam energy also revealed some limitations to the generator volt meter (GVM) that is used to regulate the Pelletron high voltage. Figure 5 shows the time evolution of the Pelletron voltage (average value being subtracted) as measured by the GVM, a capacitive pickup (CPO) and the displacement at R01. Both the CPO and the R01 BPM indicate a ~ 1 kV voltage drop of several seconds at $t \approx 60$ s, while the GVM remains unperturbed. This could be the result of micro-discharges with nano-Amperes current flowing directly to the GVM plate and we are considering implementing a magnetic shielding of the GVM. Note that at this time, the CPO signals are not used for regulation of the high voltage.

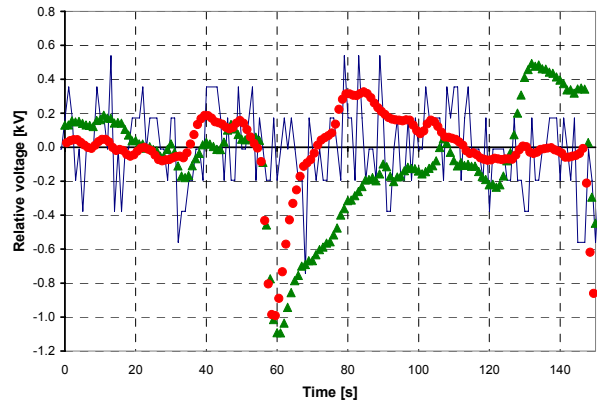


Figure 5: Relative (AC) Pelletron voltage as a function of time. Blue: GVM; Red circled: Capacitive pickup (CPO); Green triangles: position at R01.

Because these drops in voltage are of short period of times, their impact on cooling is low. However, they can

be a problem during drag rate measurements by the voltage jump method.

Electron Beam Related Operational Issues

Since we started to use the electron beam for cooling, we dealt with three major issues: transverse emittance growth, fast beam loss and lifetime degradation of the antiprotons.

Transverse emittance growth was observed during the mining process where both the physical (i.e. peak current) and phase space density become relatively large [3]. A change of our operating point from 25.414/24.422 (H/V) to 25.452/24.469, suggested from the analysis of quadrupole instabilities in the presence of an electron beam [9], eliminated almost entirely the emittance growth problem. However, we now believe that the quadrupole instability was not the mechanism by which emittance growth was induced but rather a single particle resonance mechanism [10], which could also explain the different beam lifetime observed for different working points in tune space [11].

Fast antiprotons loss is typically the result of one of two different beam conditions, both of which become more difficult to avoid as the number of antiprotons increases: high phase-space density or high peak current of the antiproton beam. With the addition of dampers [12], the threshold for resistive wall dipole instabilities [13] has greatly increased [11] and has not been an issue recently. To deal with high peak currents occurring during mining of large stacks, the RF structure of the mined buckets has been modified [14], reducing by a factor of 2 the maximum peak current of any single bunch. The new RF structure allowed to successfully mine and extract up to $\sim 450 \times 10^{10}$ antiprotons.

Because of the problem related above with our beam current monitor, no recent observations were made regarding the lifetime degradation of the antiproton beam undergoing electron cooling. It is clear, however, that it remains the biggest issue when the number of antiprotons in the Recycler exceeds $350\text{-}400 \times 10^{10}$. It is also important to note that the history of how the antiproton beam is cooled (i.e. relative position of the electron beam w.r.t. the antiproton beam as a function of time) leads to very different lifetimes for nearly the same antiproton beam parameters. As was noted in Ref. [3], the lifetime appeared to improve at the new tunes, although no good explanation has been developed as for why. In that respect, exploring other tune regions may prove to be beneficial. Thus, additional quadrupoles are being installed in the Recycler to increase its tune phase-space range.

We are also investigating a novel procedure for cooling which relies on a modified RF bucket structure, the so-called compound bucket, which separates in the longitudinal direction the high transverse emittance, high momentum spread particles (i.e. hot particles) from the low transverse emittance, low momentum spread particles (i.e. cold particles). Then, gated stochastic cooling is applied on the hot particles, while the electron beam

remains on axis cooling more efficiently the cold particles. Details of this technique are presented in Ref. [15] along with preliminary results. The purpose of this procedure would be to provide strong cooling while maintaining a good lifetime.

COOLING PERFORMANCE

Longitudinal Cooling Force

The cooling properties of the electron beam are first evaluated with drag rate measurements by a voltage jump method [16]. Details on the methodology and results of these measurements can be found in Ref. [3], and more recent measurements of the drag force as a function the antiproton momentum offset $p \equiv P - P_0 = \gamma M_p V_{pz}$ are plotted on Figure 6. For $p \approx 4$ MeV/c, the typical rms momentum spread of the antiproton beam during operation, the drag rate ranges from 25 to 50 MeV/c per hour. This difference appears to be correlated to the transverse emittance of the antiproton beam. For the measurements presented in Ref. [3], the antiproton transverse emittance was relatively large ($2\text{-}6 \pi$ mm mrad, 95%, normalized, measured with a Schottky detector) and not accurately monitored during the data acquisition. In Figure 6, the starting initial transverse emittances, as measured with flying wires, are similar for both data sets ($< 0.5 \pi$ mm mrad, 95%, normalized). However, for the blue diamond data points, the extent of the antiproton beam in the transverse direction was further limited with a scraper, which was moved in between each measurement.

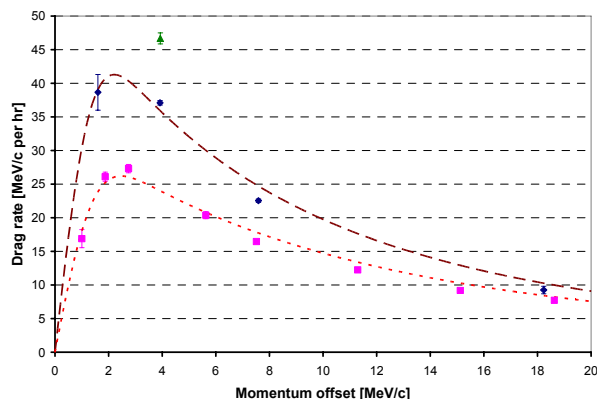


Figure 6: Longitudinal cooling force (negated) as a function of the antiproton momentum deviation. Points are data with error bars representing the statistical error (1σ) of the measurement procedure. Dashed lines are a fit to the data using a non-magnetized model. Pink squares: no scraper limiting the aperture; Blue diamonds: Scraper was brought in to the same transverse location between measurements; Green triangle: Measurement immediately after moving in and out the scraper. For all measurements, transverse stochastic cooling was applied, $I_b = 100$ mA, on-axis.

Because of various calibration issues, it is difficult to relate the acceptance limitation technique to a quantitative

measure of the emittance. Nonetheless, the data point at 46.9 MeV/c per hour obtained immediately after a scrape shows the extreme sensitivity of the friction force to the transverse distribution of the antiproton beam. More details on the friction force measurements, their interpretation and comparison with non-magnetized models can be found in Ref. [17].

Correlation to the Electron Beam Properties

The electron beam cooling capability depends on the beam energy spread σ_E , rms value of the electron angles in the cooling section θ_e , and beam current density J_{cs} (or beam size at a fixed beam current). As such, one would expect to be able to correlate the drag rate measurements with the electron beam parameters independently measured [3,8,11,18].

Fitting the data from Figure 6 with the usual non-magnetized model [19,20] does not lead to any significant disagreement (to within a factor of two) with previously reported fitted parameters [3, Table 2]. In fact, at 1.0 A cm^{-2} (for both curves in Figure 6), the fitted current density is closer to the theoretical calculation than previously reported. Also, the fitted rms electron angle is 150 and 120 μrad for the brown and red curves, respectively, which could be explained by the fact that the smaller antiproton beam experiences a better quality beam on average. On the other hand, the fitted rms energy spread (600-650 eV) is quite larger than what we would expect from the Pelletron HV ripple, $\delta U = 250 \text{ eV}$ rms and multiple-coulomb scattering and electron beam density fluctuations [21] which are estimated to contribute $\sim 100 \text{ eV}$, added in quadrature.

However, it should be noted that the extraction of the friction force F from the drag rate measurements assumes that the second derivative of the friction force w.r.t. p is small so that $F(p) \approx \dot{p}$. This latter assumption becomes questionable with the increasing amplitude of the maximum friction force and a more complex analysis of the drag rate data is being considered.

Preliminary Measurements with a Scintillator Screen

Although the cooling performance proved that the beam quality was overall adequate for regular operation, we still lack a consistent model which would explain all of our measurements.

Firstly, the beam size measured with scrapers was ~ 1.4 time larger than expected based on conservation of the magnetic flux (Bush's theorem) [8]. On the other hand, friction force measurements showed that the effective electron beam radius was much smaller than both the direct measurement with scrapers and the expected value [18], of the order of 1 mm. In Ref. [3], it was pointed out that our estimation of the envelope scalloping could be an underestimate for the core particles, which could explain the smaller measured effective radius. We also proposed that secondary electrons be responsible for the larger than expected beam

size [8]. In addition, during the optics optimization process, we observed that the cooling force had a shallow maximum when plotted against the matching solenoid strength just upstream of the cooling section. This was unexpected considering that they should affect the electron beam envelope considerably.

Preliminary measurements of the beam profile at the exit of the cooling section with a scintillator screen (a YAG crystal [22]) and gated CID camera (Figure 7) revealed interesting features that would explain the inconsistencies mentioned above. First, the beam core (saturated region) is elliptical. This indicates envelope oscillations in the cooling section, hence larger scalloping angles than estimated and a faster drop of the cooling force away from the axis than if the beam was self-similar.

Second, there is a clear halo of electrons more round than its core. The boundary of the halo is what the scrapers measure, thus explaining the large radius measured by this method.

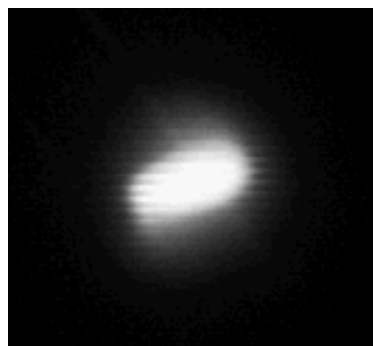


Figure 7: Picture of the electron beam at the exit of the cooling section taken with YAG screen and CID camera. The pulse amplitude was 3.2 kV (i.e. $\sim 100 \text{ mA}$).

At this time, neither the ellipticity of the distribution nor the presence of the halo is completely understood. Further measurements with OTRs and the YAG are planned for the near future.

Cooling Rates

Although friction force measurements are necessary to understand the ultimate cooling capabilities of the electron cooler, cooling rate measurements are more adequate to qualify the cooler performance for operation purposes. Cooling rates measurements were discussed in detail in Ref. [18] and typical results were found to be -8 MeV/c per hour; for the longitudinal cooling rate, $-6 \pi \text{ mm mrad/hr}$ for the average transverse cooling rate for flying wire data and $-2 \pi \text{ mm mrad/hr}$ for the average transverse cooling rate for the Schottky detector data. However, as for the drag rates, we found the cooling rates (both longitudinally and transversely) to be sensitive to the antiproton transverse emittance. This is illustrated in Figure 8, where the longitudinal cooling rate is plotted against the antiproton transverse emittance measured by flying wires.

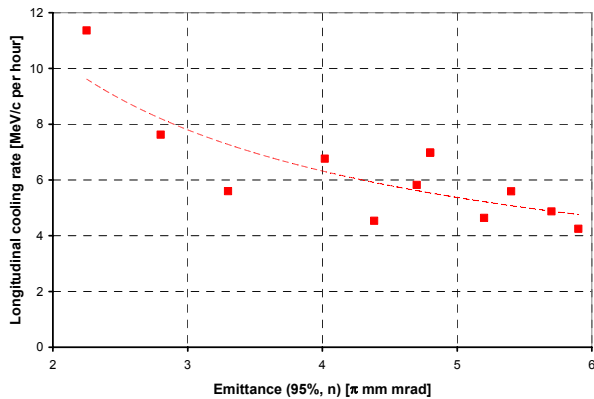


Figure 8: Longitudinal cooling rate (negated) as a function of the antiproton transverse emittance (from flying wire measurements). The dashed line is an arbitrary power law fit (for illustration only). The electron beam was on axis for all measurements (100 mA).

Once again, the image of the electron beam on the YAG screen suggests that this dependence may be due to the lack of homogeneity in the electron beam properties.

At this point, in order to assess the cooling properties of the electron beam more precisely and in an understandable fashion, the beam line optics need to be corrected. This work will take place this fall.

CONCLUSION

Electron cooling plays a preeminent role in Fermilab's latest luminosity achievements. The electron cooler high voltage stability and reliability has proven to be exceptionally good and the electron beam characteristics adequate and sufficiently stable to provide the necessary cooling performance.

Full discharges are sparse and conditioning of the accelerating columns is only required every ~ 2 -3 months. In addition, long shutdowns for Pelletron maintenance (2-3 days) are only needed every ~ 6 months.

The measured longitudinal friction force and cooling rates were found to depend greatly on the antiproton transverse emittance. Recent YAG measurements indicate that the electron beam distribution may be the main culprit. Thus, correcting the electron beam line optics could significantly improve the cooling performance further (now planned).

The antiproton lifetime under strong electron cooling remains the main issue and may be dealt with another change of the Recycler working point.

ACKNOWLEDGMENTS

We are grateful to the entire Recycler department for helping with many aspects of the work and measurements discussed in this paper and countless productive discussions.

REFERENCES

- [1] A. Shemyakin *et al.*, AIP Conf. Proc. **821** (2006) 280.
- [2] Pelletrons are manufactured by the National Electrostatics Corporation, www.pelletron.com.
- [3] L. Prost *et al.*, in Proc. of HB2006, Tsukuba, Japan, May 29-June 2, 2006, WEAY02, p 182.
- [4] 'Mining' is the first step in the extraction process that consists of capturing the core of the antiproton beam in 9 individual square buckets, leaving out the high momentum particles.
- [5] P. Derwent *et al.*, Status of the Recycler Ring, *these proceedings*.
- [6] L. Prost *et al.*, Beam-Based Field Alignment of the Cooling Solenoids for Fermilab's Electron Cooler, *these proceedings*.
- [7] L. Prost and A. Shemyakin, AIP Conf. Proc. **821** (2006) 391.
- [8] A. Shemyakin *et al.*, Proc. of EPAC'06, Edinburgh, UK, June 26-30, 2006, TUPLS069, p 1654.
- [9] A. Burov *et al.*, in Proc. of HB2006, Tsukuba, Japan, May 29-June 2, 2006, THAW07, p 334
- [10] A. Burov and V. Lebedev, in Proc. of PAC'07, Albuquerque, New Mexico, June 25-29, 2007, WEYC01, p 2009.
- [11] L. Prost *et al.*, Proc. RuPAC'06, Novosibirsk, Russia, September 10-14, 2006, WEBO02.
- [12] A. Burov, FERMILAB-TM-2336-AD (2005).
- [13] Laslett, K. Neil and A. Sessler, Rev. Sci. Instr. **36** (1965) 436.
- [14] C. Bhat *et al.*, in Proc. of PAC'07, Albuquerque, New Mexico, June 25-29, 2007, WEOCKI04, p 1941.
- [15] A. Shemyakin *et al.*, Cooling in compound buckets, *these proceedings*.
- [16] H. Danared *et al.*, Phys. Rev. Lett. **72** (1994) 3775.
- [17] A. Shemyakin *et al.*, Electron Cooling in the Recycler Cooler, *these proceedings*.
- [18] L. Prost and A. Shemyakin, in Proc. of PAC'07, Albuquerque, New Mexico, June 25-29, 2007, TUPAS030, p 1715.
- [19] Ya.S. Derbenev and A.N. Skrinsky, Particle Accelerators **8** (1977) 1.
- [20] S. Nagaitsev *et al.*, Phys. Rev. Lett. **96**, 044801 (2006).
- [21] A. Burov *et al.*, AIP Conf. Proc. **821** (2006) 159.
- [22] A. Warner *et al.*, Proc. of DIPAC'07, Venice, Italy, May 20-23, 2007, WEPB18, *to be published*.